Military Technical College
Kobry El-Kobbah,
Cairo, Egypt.

13th International Conference on Applied Mechanics and Mechanical Engineering.

INPUT SHAPING TECHNIQUES FOR LIQUID SLOSH SUPPRESSION

ABOEL-HASSAN** A., ARAFA** M. and NASSEF*** A.

ABSTRACT

The need for fast maneuvering and accurate positioning of flexible structures poses a control challenge. The inherent flexibility in these lightly damped systems creates large undesirable residual vibrations in response to rapid disturbances. Several control approaches have been proposed to tackle this class of problems, of which the input shaping technique is appealing in many aspects.

While input shaping has been widely investigated to attenuate residual vibrations in flexible structures, less attention was granted to expand its viability in further applications. The aim of this work is to develop a methodology for applying input shaping techniques to suppress sloshing effects in open moving containers to facilitate safe and fast point-to-point movements. The liquid behavior is modeled using finite element analysis. The input shaper parameters are optimized to find the commands that would result in minimum residual vibration. Other objectives, such as improved robustness, and motion constraints such as deflection limiting are also addressed in the optimization scheme. Numerical results are verified on an experimental setup consisting of a small motor-driven water tank undergoing rectilinear motion, while measuring both the tank motion and free surface displacement of the water. The results obtained suggest that input shaping is an effective method for suppressing residual liquid vibrations.

KEY WORDS

Input shaping, sloshing, genetic algorithm

** Assistant Professor, Mechanical Engineering Department, American University in Cairo, Egypt

*** Associate Professor, Mechanical Engineering Department, American University in Cairo, Egypt

INTRODUCTION

The response of lightly damped flexible structures to rapid disturbances, as in point-to-point maneuvering, usually entails large undesirable residual vibrations which may degrade the positioning accuracy and may even be severe enough to cause safety hazards, as in the transport of molten metal in ladles, for instance. In gantry cranes, one way to maintain vibrations within tolerable limits is to drive these systems at low speeds, often lower than the capability of their motors only to limit the sway of the payload. In other applications, considerable time can be wasted in waiting for residual vibrations to die out before the next motion command can safely be issued.

Numerous techniques are reported in the literature addressing the control of flexible structures to produce fast and accurate maneuvering while damping their undesirable dynamics, of which the input shaping technique is attractive in many aspects and hence will be the focus of the present study. Input shaping—also known as command shaping—has received considerable attention since its formal introduction by the seminal work of Singer and Seering [1]. The method proved successful in reducing residual vibrations in flexible structures such as gantry cranes and satellite antennas. The main idea behind input shaping is utilizing the flexible modes of the system to cancel residual vibration by convolving the reference command with set of self destructive impulses to achieve the desired motion while maintaining a low level of residual vibration at the end of the control command. One main advantage of input shaping, being a feedforward scheme, is that no sensor feedback is required. However, as in all feedforward approaches, the method is sensitive to modeling errors and parameter variation. This has prompted research into enhancing insensitivity and utilizing adaptive input shaping [2]. Other research fronts include incorporation of the system nonlinearities in the shaper design [3], hybridization of input shaping with other control techniques [4], the addition of motion constraints [5] and the application of input shaping to novel systems and models [6].

While input shaping has extensively been investigated to attenuate residual vibrations in flexible structures, less attention was granted to expand its viability in further applications, particularly problems involving fluid—structure interaction. In this context, we mention the work of Terashima and Yano [7] who applied the technique to reduce the sloshing of molten metal in the tilting ladle of a casting production line. Reference is also made to the work of Feddema *et al.* [8] which addressed slosh suppression in moving tanks by input shaping through controlling a robot arm movements.

The aim of the present work is to investigate the use of input shaping to reduce sloshing of liquids in moving containers, accounting for practical system nonlinearities and fluid motion constraints. The liquid sloshing is studied using a finite element model, which is combined with a dynamic model of a motor-driven tank to yield a set of ordinary differential equations that describe the fluid—structure interaction and that can easily be integrated numerically to obtain the time response. Adopting this methodology facilitates handling significant nonlinearities such as friction and motor saturation. Furthermore, the use of finite elements to model the liquid domain enables imposing motion constraints, such as limits for the free surface liquid displacements to prevent spilling during maneuvers, as these displacements can directly be obtained from the system degrees of freedom, unlike treatments of liquid motion by simplified mechanical mass—spring elements or pendulums. Complexities arising from the liquid response being multimodal, in addition to the imposed deflection limits and nonlinearities, prohibit

solving for the input shaper parameters in closed-form. Accordingly, an optimization scheme based on a genetic algorithm is devised to obtain the optimum commands to minimize residual vibration. Issues regarding robustness of the shaper are addressed and the findings of the numerical model are verified experimentally. The contribution of the present work lies in the comprehensive treatment of the problem at hand and in illustrating how input shaping can effectively be used to suppress residual vibrations in practical liquid—tank systems.

The remainder of this paper is organized into three sections. In Section 2, a mathematical model is formulated to simulate the dynamics of the system under investigation. The model is also verified experimentally on a motor-driven cart carrying a water tank. A procedure using a genetic algorithm is then developed in Section 3 to derive the optimum control sequence to move the tank in point-to-point maneuvers while reducing several objectives including the slosh waves and the sensitivity to modeling errors while imposing constraints regarding the free surface liquid motion. Conclusions are finally given in Section 4.

DYNAMIC MODEL AND EXPERIMENTAL WORK

Figure 1 shows a schematic diagram together with the experimental setup of the system under investigation, consisting of a rigid tank mounted on a cart that is driven by a motor through a pinion that engages with a fixed rack. The tank is partially filled with liquid to a height h_o. The length and out-of-plane width of the tank are both L. The use of input shaping to provide efficient point-to-point positioning of the tank requires determining the nature of the commands to be issued to the drive motor to fulfill these motions. The experimental setup is designed to validate the dynamic model to be developed and hence to study the tank response to optimized input shaper commands. The setup consists of a cart, driven by a DC motor, and precisely guided to undergo linear motion via linear bearings. For accurate positioning, the motor pinion meshes with a stationary rack, while the position of the cart is sensed by an optical encoder though another gear that meshes with the same rack, as indicated. A partially filled water tank measuring 10×10×10 cm is securely mounted on top of the cart. Control of the motor and the sensors feedback are handled by a personal computer using Simulink® (The Mathworks, Inc.). The water height sensor is an assembly of a float, connecting rod and optical encoder mounted on the tank wall, as shown.

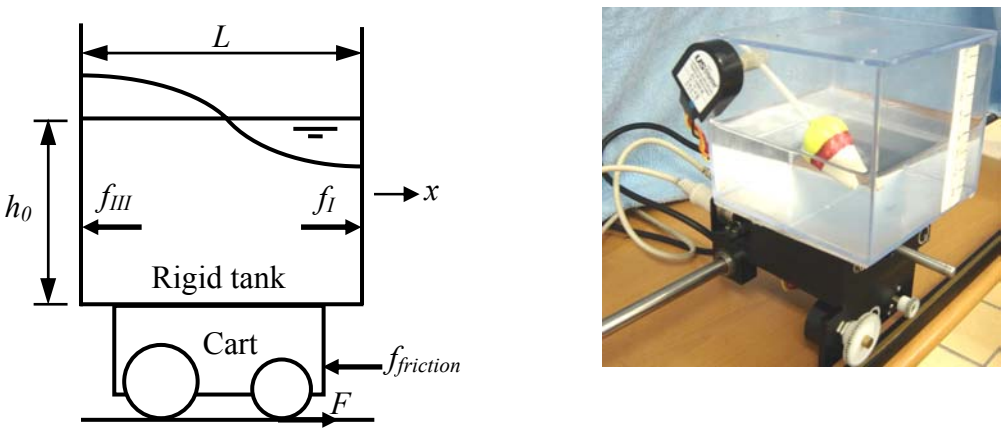

Figure 1. Schematic diagram and experimental setup of cart/tank system

FEM of Fluid—Structure Interaction

In order to derive a dynamic model that simulates the behavior of this system, the sloshing of liquids in rigid excited tanks will first be addressed to enable the calculation of the hydrodynamic forces f_I and f_{III} acting on the tank walls and the liquid surface displacement for specified tank motion. The finite element method (FEM) is conveniently adopted for this purpose. This model will then be combined with the motor dynamics and cart positioning scheme to obtain the system dynamic model. In this way, time history plots of the motor-driven tank, together with the motion of the liquid contained inside the tank, can be evaluated by numerical integration of a set of system differential equations.

The finite element model of a partially filled rigid tank undergoing lateral base motion was presented by Arafa [9] and can conveniently be adopted for the present study. The model relies upon discretizing the liquid domain into a grid of two-dimensional four-node rectangular elements with the liquid velocity potential being the only degree of freedom at each node. Effects of the liquid compressibility, viscosity and surface tension are neglected, and the motion is assumed to be irrotational allowing for potential flow. Fluid—structure interaction is handled by coupling the normal displacements of all liquid particles lying on the tank boundaries to the displacements of the tank to ensure continuity of liquid and structural motion at the liquid—tank interface.

Taking the structural and fluid degrees of freedom to be the tank wall displacements and nodal pressures, respectively, the equations governing the dynamics of fluid—structure interaction may be reproduced from [9] as:

$$\begin{aligned} \left[M_f\right]_{n\times n}\left\{\ddot{p}_f\right\}_{n\times 1}+\left\{M\right\}_{n\times 1}\ddot{x}+\left[K_f\right]_{n\times n}\left\{p_f\right\}_{n\times 1}&=\left\{0\right\}_{n\times 1}\\ m_I\ddot{x}+\left\{K_I\right\}_{1\times n}\left\{p_f\right\}_{n\times 1}&=\rho f_I\\ m_{III}\ddot{x}+\left\{K_{III}\right\}_{1\times n}\left\{p_f\right\}_{n\times 1}&=\rho f_{III} \end{aligned} \qquad (1)$$

where $\left\{p_f\right\}$ is the vector of pressure of the free surface nodes, x is the tank displacement, ρ is the liquid density, f_I, f_{III} are the hydrodynamic forces acting on the tank walls, n is the number of free surface nodes, and all other quantities pertain to the mass and stiffness matrices of the coupled liquid—tank system. Damping can easily be incorporated into the model by introducing an artificial proportional damping matrix in the equations of motion having the form:

$$\left[C\right]=\alpha\left[K_f\right] \qquad (2)$$

Motor-Cart Model

The block diagram in Fig. 2 shows the mathematical relations between the components of the numerical model. The input shaper block is responsible for changing the reference command into a shaped command that is designed to filter out the largest portion of the flexible modes of the system. The reference command is taken to be a step position signal in this study. The shaped command is compared with the actual

position of the cart, and the error signal is fed to a proportional controller whose output signal is a voltage which is fed to a DC motor. The drive force applied by the motor acts on a cart carrying a liquid-filled tank. Motion of the cart is affected by the fluid sloshing force inside the tank in addition to the force applied by the motor. The presence of the feedback is necessary for the DC motor to track the input shaper command, and not to be confused with the feedforward nature of the input shaper whose control variable is the water height in the tank.

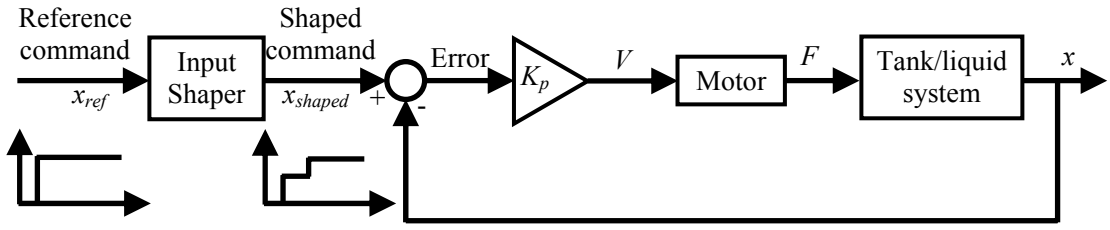

Figure 2. Numerical model block diagram

The equation relating the applied voltage, V, of the DC motor to the armature current, I_m, is given by:

$$V = I_m R_m + K_m K_g \frac{\dot{x}}{r} \tag{3}$$

where R_m is the armature resistance, K_m is the back emf constant, K_g is the reduction ratio of the motor gearbox, and r is the output pinion radius. The torque, T, and linear force, F, generated by the motor are then given by:

$$T = K_m K_g I_m = F\, r \tag{4}$$

Equations (3) and (4) can be grouped to express the resultant motor force as a function of the applied voltage and the cart linear speed as:

$$F = \frac{K_m K_g}{R_m r} V - \frac{K_m^2 K_g^2}{R_m r^2} \dot{x} \tag{5}$$

From Fig. 2, the motor input voltage can be expressed as:

$$V = K_p \left(x_{shaped} - x \right) \tag{6}$$

where x_{shaped} is the resultant position command of the shaper, K_p is the controller gain. Motor saturation is included by keeping the input voltage within maximum and minimum limits. The equation governing the cart/tank dynamics can be obtained by summing all forces acting horizontally:

$$f_I - f_{III} + F - f_{friction} = M_{cart} \ddot{x} \tag{7}$$

where M_{cart} is the cart mass and $f_{friction}$ is included in the model to account for friction forces present in the system.

System Model

Equations (1) and (7) can be used to build a complete numerical model of the system represented by the block diagram in Fig. 2. The states of the system are taken to be the linear position and the velocity of the cart, in addition to the pressure of each node of the free liquid surface and its first derivative with respect to time, hence the system state vector is:

$$\begin{Bmatrix} x_1 \\ x_2 \\ \{x_{3\to n+3}\} \\ \{x_{n+4\to 2n+4}\} \end{Bmatrix} = \begin{Bmatrix} x \\ \dot{x} \\ \{p_{f1\to n}\} \\ \{\dot{p}_{f1\to n}\} \end{Bmatrix} \tag{8}$$

The dynamic model is described by the first derivatives of the states in equation (8):

$$\dot{x_1} = x_2 \tag{9}$$

where $\dot{x_2}$ can be determined by evaluating each term of the left hand side of equation (7) and f_I and f_{III} can be obtained from the second and third rows in equation (1) as:

$$\begin{aligned} f_I &= \left(m_I \dot{x}_2 + \{K_I\}\{x_{3\to n+3}\}\right)/\rho \\ f_{III} &= \left(m_{III} \dot{x}_2 + \{K_{III}\}\{x_{3\to n+3}\}\right)/\rho \end{aligned} \tag{10}$$

The motor force, F, is determined from equations (5) and (6) while accounting for the saturation condition. For practical applications, friction is modeled as a sliding Coulomb friction force, hence:

$$F_{friction} = -\mu N \ \mathrm{sgn}(x_2) \tag{11}$$

where N is the normal load which is the combined weight of the tank and cart, and μ is the coefficient of kinetic friction. To account for static friction, an additional condition is added to set both the cart's velocity and acceleration to zero whenever the velocity drops below a certain threshold that can be determined experimentally. This condition, together with the nonlinear *sgn* function in equation (11) can more easily be incorporated in the present numerical model than in alternate closed-form solutions. Equations (5), (6), (10) and (11) can be combined together to substitute for the left hand side terms in equation (7) to solve for $\dot{x}_2$ as follows:

$$\dot{x}_2 = \frac{\rho\left(F - f_{friction}\right) + \{K_I - K_{III}\}\{x_{3\to n+3}\}}{\left(\rho M_{cart} - m_I + m_{III}\right)} \tag{12}$$

The time derivative of the third through $n+3$ states is:

$$\{\dot{x}_{3\to n+3}\} = \{x_{n+4\to 2n+4}\} \tag{13}$$

From equation (1), the time derivative of the last set of states $\{x_{n+4\to 2n+4}\}$ is:

$$\{\dot{x}_{n+4\to 2n+4}\} = \left[M_{ff}\right]^{-1}\left[\{M\}\dot{x}_2 + \left[K_f\right]\{x_{3\to n+3}\}\right] \tag{14}$$

The time derivative of the state equations (9), (12), (13) and (14) constitute the complete dynamic model that simulates the system. The displacement of the free surface nodes $\{U_{1\to n}\}$ from the undisturbed water level is given by:

$$\{U_{1\to n}\} = \{p_{f1\to n}\}/\rho g \tag{15}$$

Figure 3 shows a comparison of the numerical and experimental slosh responses for a commanded step input displacement. A 20 × 20 element mesh is used in the FE model of the liquid domain, and an artificial proportional damping matrix was added to the FE model in the form proposed by equation (2) to obtain comparable decay rates. A detailed list of system parameters can be found in [10]. Inspection of the plots reveals that the slosh responses are in close agreement. The slight discrepancies can be attributed to nonlinearities such as surface tension and viscous effects.

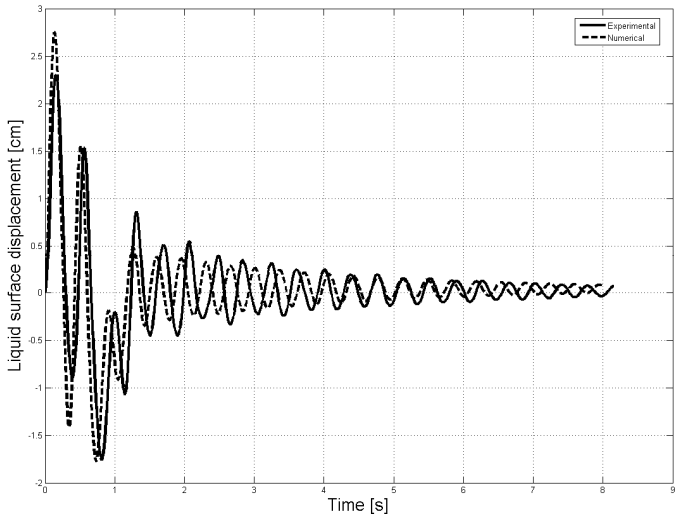

Figure 3. Numerical and experimental slosh response.
(x_{ref}= 0.6 m, K_p = 25, h_0 = 4 cm, α = 0.0025)

INPUT SHAPING DESIGN USING OPTIMIZATION

Once a dynamic model has been formulated, an optimization scheme will now be designed to obtain the input shaper parameters, namely the timing and magnitudes of the necessary commanded pulses that drive the system from one point to another while achieving certain prescribed time domain performance specifications. The methodology of input shaper design by optimization adopted herein is also based on the work of Meshreki [11]. Although input shaping design is a straightforward procedure in the case of linear systems, the presence of nonlinearities complicates this process. While sloshing may fairly be modeled to be linear, the coupling of sloshing in the present

application with the tank's motion, together with the nonlinearities inherent in the motor behavior, precludes the trivial linear solution.

Zero Vibration (ZV) Input Shaper for Sloshing

Because the Zero Vibration (ZV) shaper has only two variables, namely the time of the second impulse and the amplitude of the first impulse, these can be evaluated by enumeration of all possible combinations in the feasible range and selecting the best results by searching for the minimum value of the performance index. For simplicity the performance index is taken to be the maximum water slosh level reached after the application of the second impulse. The feasible range and the incremental steps of the enumeration should be chosen based on the specifics of the problem at hand. In this study, the value of the enumeration step of the second impulse timing (T_2) is taken equal to the digital resolution of the experimental controller (0.01s).

The experimental results for the ZV shaper designed based on enumeration is shown in Fig. 4 and the optimum shaper parameters are A_1 = 0.4, T_2 = 0.52 for a shaper designed for a liquid of 4 cm while the final desired cart displacement is 0.6 m. The plot shows both the shaped and unshaped responses for comparison. The maximum residual slosh amplitude after the motor settles in the unshaped case is 0.92 cm. This value is reduced to 0.16 cm after applying the input shaper. The reduction of the residual slosh amplitude comes at the cost of increasing the motor settling time as shown in Fig. 5 from 1.01 seconds in the unshaped case to 1.34 seconds in the shaped case.

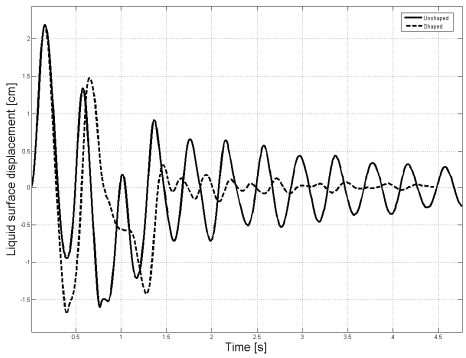

Figure 4. Experimental ZV shaper response as compared to the unshaped response.
(x_{ref}= 0.6 m, K_p = 25, h_0 = 4 cm)

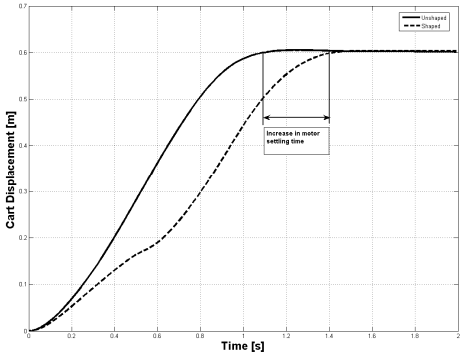

Figure 5. Experimental cart response for unshaped and shaped commands.
(x_{ref}= 0.6 m, K_p = 25, h_0 = 4 cm)

While the main advantage of ZV input shaper is the simplicity of the design procedure, this comes at the cost of increased sensitivity to modeling errors or parameters variation. As shown in [1] for a second order system, input shaper performance degrades sharply for a change of the natural frequency of a mere $\pm$3%. Linear ZV shapers are more sensitive to errors in the natural frequency than they are to errors in the damping ratio. For the case at hand, a tank filled with water up to a height of 4 cm has a fundamental slosh frequency of 2.58 Hz. While this value will increase and saturate at 2.79 Hz (8.1% increase) for appreciably high water heights, it will drop sharply for smaller heights. Consequently, a linear ZV shaper is expected to give inferior performance if designed at a water height of 4 cm and operates at smaller

heights. This is indicated in Fig. 6 which shows the numerically simulated residual vibration amplitude when applying the optimum ZV shaper designed at a height of 4 cm to actual water heights varying from 50% to 300% of the design height. The ratio of actual to design liquid height is denoted as the non-dimensional liquid height and is shown in the abscissa. The minimum value of residual slosh amplitude is at a non-dimensional height of unity, as expected. The curve almost saturates for values greater than 1 while shoots up for values less than 1.

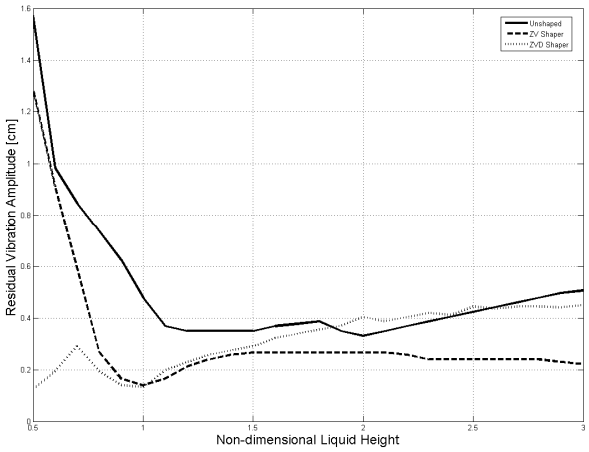

Figure 6. Residual vibration amplitude for unshaped, ZV and ZVD shapers designed at 4 cm liquid height and operating at different liquid heights (x_{ref}= 0.6 m, K_p = 25, h_0 = 4 cm)

Zero Vibration Derivative (ZVD) Input Shaper for Sloshing

The problem of shaper sensitivity has been tackled in the literature by adding an extra constraint in the design of the shaper in addition to the traditional zero vibration constraint [1]. The additional constraint is to set the derivative of the residual vibration with respect to a certain model parameter, typically the natural frequency, to zero resulting in a shaper having 3 pulses. The four variables of the ZVD shaper preclude the use of enumeration to determine the optimum shaper, therefore a more elaborate optimization scheme is employed. Because of the limited number of variables, and the expected harmonic nature of the objective function, it was decided to use real-coded genetic algorithms (GA) [12].

There are mainly two challenges in optimization problems. First, to transform the qualitative design requirements into a quantitative performance index, in order to be able to state an objective function that captures all the elements of the design requirements. Second, the optimization scheme itself has to be fine-tuned based on the characteristics of the problem at hand. The various parameters employed in the present GA scheme are listed in Table 1.

The qualitative design requirement of ZVD shaper are:

1. Creating minimum residual vibration at the design water height.
2. Should the water height decrease, the ZVD has to remain effective in suppressing the residual vibration.
3. The shaper time should be minimal to avoid the trivial solution of achieving good

Table 1. GA basic parameters used in optimization

Number of variables	4	Population size	60
Number of generations	40	Uniform mutation	4
Boundary mutation	4	Arithmetic cross over	2
Simple arithmetic	2	Whole non-uniform mutation	4
Heuristic cross over	2	None uniform mutation parameter	6
Simple cross over parameter	10	Q	0.1

residual amplitude response at the cost of increasing the motor settling time indefinitely.

The first requirement is represented by the largest magnitude of the residual sloshing after the settling of the motor, hence its objective function is stated as:

$$obj_1 = \max(U_{t=T_s}^{t=T_f}) \quad at\ h_{operating} = h_{design} \tag{16}$$

where *U* is the displacement of the surface liquid node adjacent to the tank wall in the FE model, T_s is the settling time of the motor and T_f is the final time value. This objective is taken for the case where the water level in the tank, $h_{operating}$, is equal to the water height at which the shaper is designed, h_{design}.

The second design requirement stated above has to do with the robustness of the ZVD shaper. From Fig. 6, it is evident that the ZV shaper performance, as measured by the residual vibration amplitude, deteriorates significantly in the region where the non-dimensional height is from 50% to 75%. The aim of designing a ZVD shaper is to improve insensitivity by reducing such a sharp slope. Considering the specifics of the problem at hand and the fact that it is explicitly desired to reduce the sensitivity of the sloshing in the direction of decreasing operating heights only, the second requirement's objective function is similar to the previous case with the response taken at two operating heights lower than the design height:

$$obj_2 = \max(U_{t=T_s}^{t=T_f})_{h_{operating}=0.5h_{design}} + \max(U_{t=T_s}^{t=T_f})_{h_{operating}=0.75h_{design}} \tag{17}$$

The third design requirement dealing with the settling time of the motor is represented by the increase of the settling time of the motor (T_s) in the shaped command compared to the unshaped command, and is hence expressed as:

$$obj_3 = \max\left(T_{s(shaped)} - T_{s(unshaped)}\right) \tag{18}$$

In order to add the three objective functions algebraically, they must all have comparable magnitudes, so that no one objective dominates the others. This can be done by normalizing the three objectives and adding factors to the normalized objective

function to allow the designer to give different weights for each objective. The final version of the objective function is hence given by:

$$obj = \sum_{i=1}^{3} k_i \times \frac{\max(U_{t=T_s}^{t=T_f})_{shaped} @ h = c_i \times h_{design}}{\max(U_{t=T_s}^{t=T_f})_{unshaped} @ h = c_i \times h_{design}} + k_4 \frac{\left(T_{s(shaped)} - T_{s(unshaped)}\right)}{T_{s(unshaped)}} \qquad (19)$$

where k_i is the weighting factor for each design criterion, h is the operating height, h_{design} is the water height the shaper is designed at, c_i are factors taken as [1, 0.75, 0.5]. The dashed and dotted plots of Fig. 6 show numerical run of the sensitivity of the ZV and ZVD for non-dimensional heights ranging from 0.5 to 3 together with the performance of the unshaped response. The optimum shaper parameters for this case are A_1 = 0.2, A_2 = 0.19, T_2 = 1.02, and T_3 = 1.22. The weighting factors used in the objective function of the ZVD shaper are k_1= 3, k_2=2, k_3=2, k_4=1.

It is very clear that both the ZV and ZVD are superior to the unshaped command almost over the entire range of operation. It is also clear that the designed ZVD is successful in reducing the residual vibration amplitude significantly for non-dimensional heights in the range of 0.5 to 0.75. The use of ZVD shaper is particularly advantageous in practical applications where a drop in natural frequency is likely to occur as the liquid being transported is periodically consumed or dispensed. This improvement in the performance comes at the cost of deteriorating performance for higher non-dimensional heights, however it still remains below the unshaped command response. This deterioration is expected since no factor of the objective function reflects the performance of the ZVD shaper in that range. Figure 7 shows a numerical comparison of the unshaped, ZV and ZVD responses where the input shapers are designed at a water height of 4 cm and operating at an actual height of 3 cm. The least residual vibration is observed for the ZVD shaper, as intended.

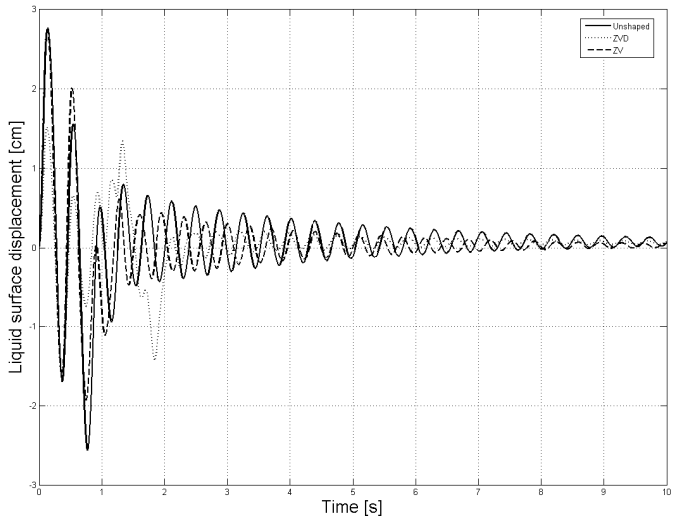

Figure 7. Numerical comparison of unshaped, ZV and ZVD shaper responses.

Deflection Limiting Input Shaper for Sloshing

The convenience of the numerical model and shaper design using optimization make the addition of more objectives and motion constraints very attractive. One constraint repeatedly addressed in the literature is Deflection Limiting (DL) [13] in which the maximum magnitude of structural deflection is limited to a certain predefined value. This constraint is useful for applications that involve partially filled moving tanks since it may be desired to prevent spilling during motion.

In the optimization scheme, DL can be expressed as a constraint, where a penalty is applied to the objective function should the maximum amplitude of vibration of any of the FE nodes exceeds a predefined value. Since DL is a hard constraint, the weighting factors suggested in equation (19) have to be chosen carefully to relax other objectives in favor of the constraint. For example, it is expected that the DL constraint would cause the settling time of the motor to increase. Physically, this means that requiring fast motor maneuvers with limited liquid slosh are two contradicting objectives, thus one of them has to be relaxed to be able to accomplish the other. In the experimental run shown in Fig. 8 the maximum (positive) amplitude of vibration was limited to 1 cm. The optimum shaper parameters for this case are A_1 = 0.167, A_2 = 0.22, T_2 = 0.22, and T_3 = 0.44 and the weighting factors used in equation (19) are k_1 = 3, k_2= 1, k_3 = 1, k_4 = 0.5. Comparing the DL response of Fig. 8 with the unshaped response indicates that the adopted input shaping technique can successfully reduce the maximum amplitude of sloshing from 2.3 cm to 0.95 cm and reduce the maximum residual sloshing from 0.9 cm to 0.15 cm. The improved performance comes at the mere cost of 0.42 seconds increase in the motor rise time [10]. For comparison, the shaped input commands are shown in Fig. 9.

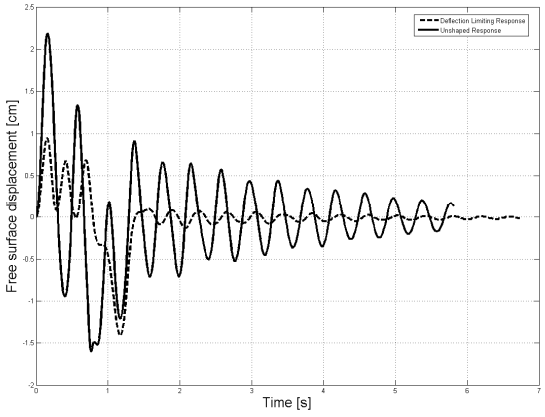

Figure 8. Experimental response of the DL shaper as compared to the unshaped response. (x_{final} = 0.6 m, K_p = 25, h_0 = 4 cm)

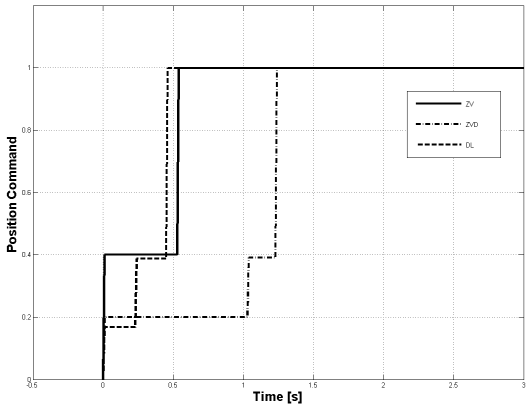

Figure 9. Shaped input commands

CONCLUSIONS

This work demonstrated both theoretically and experimentally how input shaping techniques can effectively be applied to mitigate sloshing effects in open liquid tanks undergoing point-to-point maneuvers. The system dynamics were modeled numerically, taking into consideration motor saturation and friction. The input shaper parameters

were optimized to find the commands that would result in minimum residual vibration. The objectives were to minimize residual vibration, as well as the motor settling time. The two main input shaping techniques addressed in this work were the Zero Vibration (ZV) and Zero Vibration Derivative (ZVD) schemes. Both demonstrated improved performance over unshaped commands. While ZV was capable of reducing residual vibration by nearly 80%, its sensitivity was outperformed by the ZVD scheme, which showed a larger range of acceptable performance allowing more room for modeling errors and parameter variation. The concept of deflection limiting, originally developed in the literature to minimize structural swaying during commanded motion, was implemented herein to limit the amplitude of liquid sloshing over the entire length of the tank motion, thus reducing the chances of spilling.

REFERENCES

[1] N.C. Singer and W.P. Seering, Preshaping command inputs to reduce system vibration, *Journal of Dynamic Systems, Measurement and Control,* 112 (1990) 76-82.

[2] C. F. Cutforth, and L.Y. Pao, Adaptive Input Shaping for Maneuvering Flexible Structures, *Automatica* 40 (2004) 685-693.

[3] K. Sorensen and W. Singhose, Oscillatory Effects of Common Hard Nonlinearities on Systems Using Two-Impulse ZV Input Shaping, *Proceedings of the 2007 American Control Conference*, (2007) 5539-5544.

[4] Z. Mohamed, and M.O. Tokhi, Hybrid Control Schemes for Input Tracking and Vibration Suppression of a Flexible Manipulator, *Proceedings of the Institution of Mechanical Engineers*, Part I, Journal of Systems and Control Engineering 217 (1) (2003) 23-34.

[5] W. Singhose, A. Banerjee and W. Seering, Slewing Flexible Spacecraft with Deflection-Limiting Input Shaping, *Journal of Guidance, Control, and Dynamics*, 2 (1997) 291-298.

[6] A.K. Banerjee, Dynamics and Control of the WISP Shuttle-Antennae System, *Journal of Astronautical Sciences* 1 (1993) 73-90.

[7] K. Terashima and K. Yano, Sloshing analysis and suppression control of tilting-type automatic pouring machine, *Control Engineering Practice*, 9 (2001) 607-620.

[8] J. Feddema, C. Dohrmann, G. Parker, R. Robinett, V. Romero and D. Schmitt, A comparison of maneuver optimization and input shaping filters for robotically controlled slosh-free motion of an open container of liquid, *Proceedings of the 1997 American Control Conference*, 3 (1997) 1345-1349.

[9] M. Arafa, Finite element analysis of sloshing in rectangular liquid-filled tanks, *Journal of Vibration and Control*, 13 (7) (2007) 883-903.

[10] A. Aboel-Hassan, *Design and optimization of input shapers for liquid slosh suppression*, Masters Thesis, American University in Cairo, Egypt, 2007.

[11] M. A. H. Meshreki, *Design methodology for input shapers using genetic algorithms in flexible nonlinear systems*, Masters Thesis, American University in Cairo, Egypt, 2004.

[12] F. Herrera, M. Lozano and , M. and J.L. Verdegay, Tackling real-coded genetic algorithms: operators and tools for behavioral analysis, *Artificial Intelligence Review* 12 (1998) 265-319.

[13] W. Singhose, A. Banerjee and W. Seering, Slewing flexible spacecraft with deflection-limiting input shaping, *Journal of Guidance, Control, and Dynamics*, 2 (1997) 291-298.